PAPER

A novel flexible cuff-like microelectrode for dual purpose, acute and chronic electrical interfacing with the mouse cervical vagus nerve

To cite this article: A S Caravaca *et al* 2017 *J. Neural Eng.* **14** 066005

IOP Publishing Journal of Neural Engineering
J. Neural Eng. **14** (2017) 066005 (10pp) https://doi.org/10.1088/1741-2552/aa7a42

A novel flexible cuff-like microelectrode for dual purpose, acute and chronic electrical interfacing with the mouse cervical vagus nerve

A S Caravaca[1,6], T Tsaava[2,6], L Goldman[3,6], H Silverman[2], G Riggott[4], S S Chavan[2], C Bouton[3], K J Tracey[2,3], R Desimone[4,7], E S Boyden[5,7], H S Sohal[3,7] and P S Olofsson[1,7]

[1] Department of Medicine, Solna, Karolinska Institutet, Center for Molecular Medicine, Center for Bioelectronic Medicine, Karolinska University Hospital, Stockholm, Solna, Sweden
[2] Feinstein Institute for Medical Research, Laboratory of Biomedical Science, Manhasset, NY, United States of America
[3] Feinstein Institute for Medical Research, Center for Bioelectronic Medicine, Manhasset, NY, United States of America
[4] Massachusetts Institute for Technology, Cambridge, MA, United States of America
[5] Media Lab, Massachusetts Institute for Technology, Cambridge, MA, United States of America

E-mail: peder.olofsson@ki.se and hsohal@northwell.edu

Received 31 January 2017, revised 2 June 2017
Accepted for publication 19 June 2017
Published 1 November 2017

Abstract

Objective. Neural reflexes regulate immune responses and homeostasis. Advances in bioelectronic medicine indicate that electrical stimulation of the vagus nerve can be used to treat inflammatory disease, yet the understanding of neural signals that regulate inflammation is incomplete. Current interfaces with the vagus nerve do not permit effective chronic stimulation or recording in mouse models, which is vital to studying the molecular and neurophysiological mechanisms that control inflammation homeostasis in health and disease. We developed an implantable, dual purpose, multi-channel, flexible 'microelectrode' array, for recording and stimulation of the mouse vagus nerve. *Approach.* The array was microfabricated on an 8 μm layer of highly biocompatible parylene configured with 16 sites. The microelectrode was evaluated by studying the recording and stimulation performance. Mice were chronically implanted with devices for up to 12 weeks. *Main results.* Using the microelectrode *in vivo*, high fidelity signals were recorded during physiological challenges (e.g potassium chloride and interleukin-1β), and electrical stimulation of the vagus nerve produced the expected significant reduction of blood levels of tumor necrosis factor (TNF) in endotoxemia. Inflammatory cell infiltration at the microelectrode 12 weeks of implantation was limited according to radial distribution analysis of inflammatory cells. *Significance.* This novel device provides an important step towards a viable chronic interface for cervical vagus nerve stimulation and recording in mice.

Keywords: vagus nerve stimulation, inflammation, peripheral nerve, bioelectronic medicine, neural reflex, homeostasis, conduction velocity

(Some figures may appear in colour only in the online journal)

[6] First co-authors.
[7] Authors to whom any correspondence should be addressed.

Introduction

Bioelectronic medicine, an emerging interdisciplinary field, brings molecular biology and neurotechnology together to use electrical devices as therapeutic agents to treat disease by targeting specific molecular mechanisms through delivery of electrical impulses to defined neural circuits [1–3]. There is increasing evidence that neural reflex circuits modulate innate and adaptive immunity [4]. The 'inflammatory reflex' is a neural circuit in which action potentials transmitted in the vagus nerve play a key role to regulate inflammation [5, 6]. This pathway can be activated by electrical stimulation of the cervical vagus nerve. Vagus nerve stimulation significantly attenuates pro-inflammatory cytokine levels in experimental disease, and murine disease models have been used to map the neurophysiology of the efferent arc of the inflammatory reflex in detail [7, 8]. The resulting discoveries have spawned human clinical trials using implanted devices for electrical stimulation of the vagus nerve for treatment of chronic diseases such as rheumatoid arthritis and Crohn's disease with encouraging results [9, 10].

However, the optimal parameters for vagus nerve stimulation in inflammatory diseases have not been established, in part because technology for chronic implantation of electrodes in relevant mouse models has been lacking. For the same reason, the neurophysiology of long-term electrical vagus nerve stimulation has not been mechanistically addressed. It is likely that electrodes suitable for chronic implantation in mice would significantly improve our ability to optimise stimulation parameters in chronic inflammatory diseases.

In addition, little is known about the electrical activity in the sensory, afferent arc of the inflammatory reflex. The vagus nerve relays signals on cytokine levels in the periphery to the central nervous system [11, 12], but studying the neurophysiology of these afferent signals has been challenging. Recent discoveries suggest that the vagus nerve transmits action potentials of specific neural signatures in response to specific cytokines [13]. Chronic electrode implants capable of recording detailed electrical activity of the vagus nerve would enable testing the hypothesis that defined inflammatory conditions elicit identifiable electrical signatures in the vagus nerve [1, 13].

Mice have long served as experimental models in understanding disease pathology and have propelled discovery of molecular mechanisms underlying the onset of disease, which is a key step in improving prevention and treatment of disease. A microelectrode for chronic use with the capacity for both electrical stimulation and recording would support further expansion of our knowledge of potential neural control of disease pathogenesis over time, and electrical activity in the nerve.

Many current electrode designs have low channel counts allowing the capture of only a certain number of compound action potentials (CAPs) to any given challenge of the nerve. Further, many of these electrodes can not be successfully implanted chronically due to their size, and risk damaging the nerve over time [14]. Optimally, chronic implants should both allow for repeated measurements of electrical activity and repeated electrical stimulation of the nerve in health and disease.

The design challenges of interfacing with the mouse cervical vagus nerve includes successfully wrapping around a cuff that causes minimal damage to the nerve and ensures good electrical contact. Further, routing the connections from the electrodes to an appropriate connector, without placing unnecessary tethering forces on the nerve to avoid damage over time is another challenge.

A microfabrication process was already developed for flexible, highly biocompatible probes intended for intracortical use and capable of stably recording electrical activity in the rabbit cortex for a period exceeding two years [15–17]. To our knowledge, this technology has not yet been implemented for interfacing with peripheral nerves. Here, we set out to use the thin film parylene-C microfabrication technology for development of a multichannel microelectrode suitable for chronic implantation, electrical stimulation, and recording of electrical activity in the mouse vagus nerve.

Materials and methods

The 16 electrode sites were configured on a 2 mm × 3 mm, 8 μm thick parylene sheet in different arrangements. The electrodes were spaced in a 350 μm wide region to accommodate for the circumference of the mouse cervical vagus nerve, which commonly is ~350–380 μm. Electrode site areas were 6400, 2500 or 225 μm^2. The arrangement of electrode sites were either tetrode-like (figure 1(A)) or diagonal (figure 1(B)). The oversize flap design facilitates ease-of-handling during surgery and secure placement of the device in the mouse. In some designs, two macro-stimulation sites were placed at either end of the microelectrode with recording sites located in between.

To mechanically decouple the microelectrode from the larger interfacing ribbon cable (3 cm long, 3 mm wide), the design has a 'necking region' to accommodate the movement of the nerve relative to the microelectrode and attenuate long-term insult to the nerve. The ribbon cable contains bond pads that allows interfacing to commercial Omnetic nanoseries connectors (NPD-18-AA-GS, Omnetics Corporation, USA) used to interface with electrophysiological set-ups (figure 1(C)).

Electrode microfabrication and wiring

Electrode microfabrication followed previously optimised process flows used for parylene-C and tungsten-titanium (WTi) technology [15, 16]. In short, the microelectrode consists of a parylene-C (4 μm)-WTi (300 nm)-parylene-C (4 μm) sandwich. WTi was etched with SF_6 reactive ion etch (RIE) to define the metal traces, electrode sites and bondpad regions. The parylene-C insulating layers were simultaneously etched using O_2 RIE to define the overall body of the electrode and to re-open the recording sites and bondpad regions.

For device release from the carrier wafer previous process flows used aluminum etched by TMAH. However, in this generation, HF (1:10 49% HF) released devices a lot faster (typically under 1 min), to minimise the exposure of the parylene-C

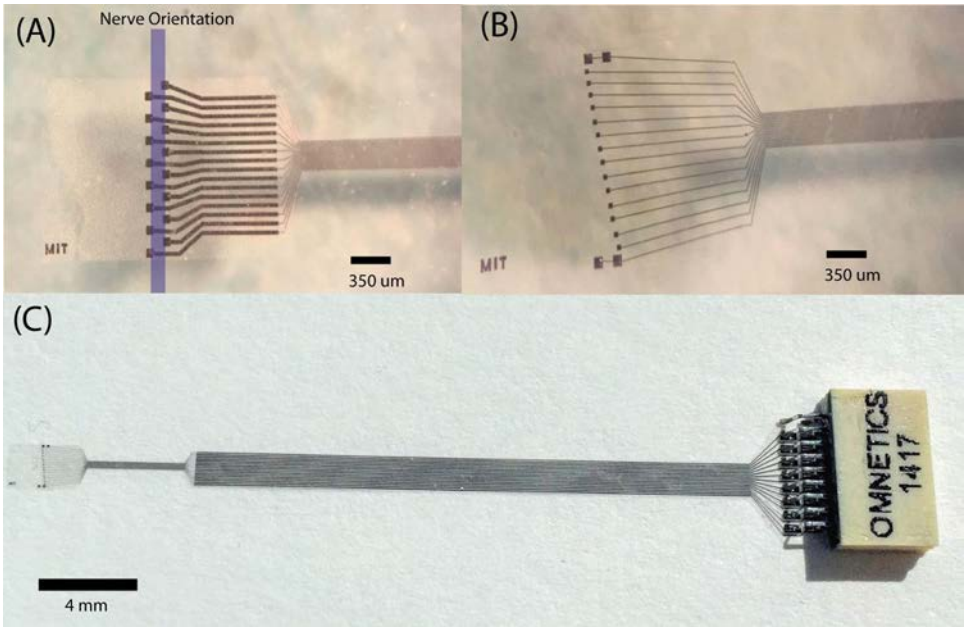

Figure 1. Microelectrode designs for peripheral nerves in the mouse. (a) A tetrode like electrode format with a blue line showing the direction of the nerve. Recording site area 6400 μm^2. The oversized flap wraps around the nerve and is secured in place with the use of sutures. (b) The diagonal format of recording sites (2500 μm^2) with two macro stimulation sites (6400 μm^2) at either end. (c) The microelectrode shown with incorporated ribbon cable and connector.

based devices to wet etchants, which could cause abnormalities in the layers (e.g. polymer swelling) [16].

Connectors were bonded to the corresponding WTi bondpads under a stereoscope. Silver epoxy was applied to the connector, aligned and placed on the metal bondpads [16]. Successful electrical connections were confirmed through impedance measurements at 1 kHz in physiological saline using an IMP 2C impedance meter (Microprobes, USA). The connector was insulated using two-part epoxy.

Ethics statement

This study and all experimental protocols were approved by the Institutional Animal Care and Use Committee (IACUC) at the Feinstein Institute for Medical Research, Northwell Health System (Manhasset, NY, USA), which follows the National Institute of Health (NIH) guidelines for the ethical treatment of animals, and by the Stockholm Regional Board for Animal Ethics (Stockholm, Sweden).

Animals

We used male BALB/c (aged 8–12 weeks) and C57Bl/6J (8–12 weeks) mice purchased from Charles River Laboratories. They were housed in a laboratory environment on a 12 h light and dark cycle at 25 °C, with *ad libitum* access to food and water.

Microelectrode implantation

Following induction of anesthesia with isoflurane, mice were placed in supine position and a ventral midline cervical incision was performed between the mandible and sternum. Subcutaneous tissues were retracted laterally to expose the salivary glands. A gauze pad was placed over the incision and mice were placed in prone position. A dorsal midline incision was made and subcutaneous tissues were retracted laterally. The integrated cable was subcutaneously tunneled from the back of the mouse back towards the midline cervical incision. The mouse was placed back into the supine position and the salivary glands were bluntly separated and retracted away from the operative field. Further blunt dissection revealed the left neurovascular bundle containing the cervical vagus nerve, which was dissected away from the vasculature and isolated between the sternomastoid and sternohyoid muscles, and a suture placed under the nerve to facilitate electrode placement. The microelectrode was placed under the nerve, folded over and sutured to secure its place. The connector was fixed to the head of the mouse. Mice subsequently recovered on a heating pad until they gained adequate righting reflex and returned to the home cage.

Vagus nerve stimulation

Electrical stimulation of the left cervical vagus nerve was performed using a stimulation module (Plexon, TX, USA) set at current control, 1 mA, 250 μs biphasic pulse, 50 μs interphase delay, 10 Hz, for 60 s. Mice in the sham group were subjected to surgery, but no electrical stimulation. After 3 h of recovery, 5 mg kg^{-1} endotoxin was administered intraperitoneally (endotoxin from *Escherichia coli*, 0111:B4; Sigma-Aldrich, MO, USA). Mice were euthanized 90 min post-injection and serum was analysed for levels of tumor necrosis factor alpha (TNFα) by ELISA (R&D Systems) according to manufacturer instructions.

In vivo recording

In spontaneously breathing mice under isoflurane anesthesia, electrical activity was sampled at 30 kHz using a RHD 2000 evaluation system (Intan Technologies, USA) using a unipolar

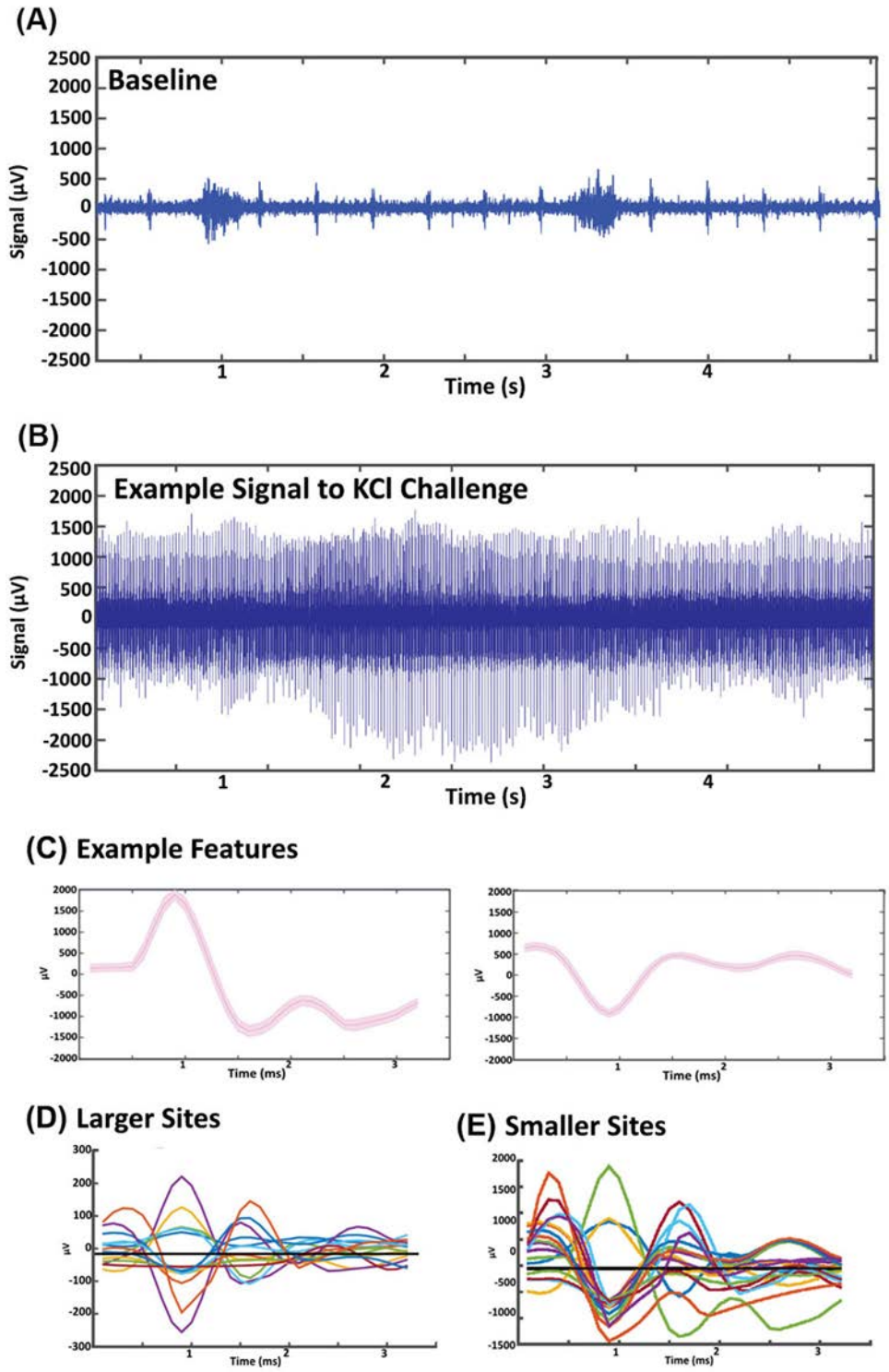

Figure 2. Electrical activity in response to potassium chloride (KCl). Anesthetized mice were implanted with a microelectrode on the left cervical vagus nerve. Data was continuously acquired at 30 kHz sampling rate. (A) Example of 200 Hz high passed signal of recorded baseline activity. Burst activity synchronous with pulse and respiration was observed. (B) Example of 200 Hz high passed signal of vagus nerve activity upon cervical vagus nerve exposure to 4 mM KCl. (C) Representative features extracted from the raw signal recording upon KCl challenge. (D) Mean waveforms of CAPs extracted from activity recorded at the 6400 μm^2 recording sites. (E) Mean waveforms of CAPs extracted from activity recorded at 2500 μm^2 recording sites.

recording set-up, with the reference wire placed in the contralateral salivary gland. A software 200 Hz high-pass filter was applied to the active channels, and the 'spike-scope' feature in the bundled software used for real-time visualisation of CAPs. Baseline activity was acquired for 30 min. Under isoflurane, the heart rate was 370 beats $min^{-1} \pm 20$ and respiratory rate was 54 breaths $min^{-1} \pm 7$. During continuous acquisition, mice were subjected to (1) 50 μl of potassium chloride (KCl; 4 mM) application directly on top of the vagus nerve with a parafilm trough underneath the nerve to prevent

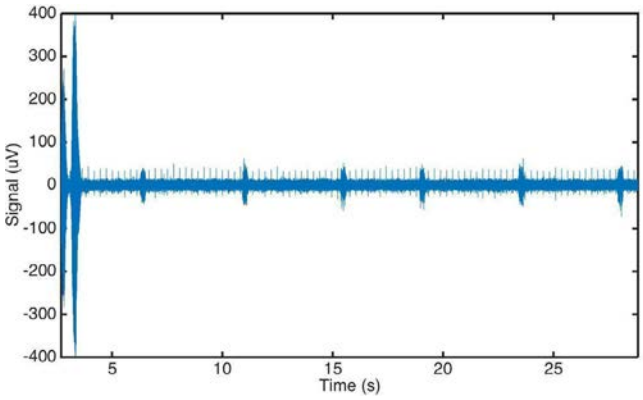

Figure 3. Electrical cervical vagus nerve activity following intraperitoneal injection of saline. Anesthetized mice were implanted with a microelectrode on the left cervical vagus nerve. Data was continuously acquired at 30 kHz sampling rate. Injection was performed at time '0'. A movement artifact from the injection is visible in the first 5 s post-injection.

spreading to other structures, (2) intraperitoneal injection of 200 μl of physiological saline or (3) intraperitoneal injection of 200 μl of interleukin-1β (IL-1β; 350 ng; eBioscience, CA) in physiological saline.

Recorded raw data was imported into Offline Sorter (Plexon, USA), where a 200 Hz high pass filter was applied to extract the frequency band of interest for CAPs. Principal component analysis (PCA) was utilised for CAP sorting. A threshold crossing was set to capture most of the potential CAPs and include some 'noise' to supply a defined noise profile in the PCA space to contrast with identified features. The threshold level was set by taking the median of the mean bandpassed signal/0.6745 (σ). The threshold was set at 4σ [19]. Saved features, including waveforms and 'spike' timings, were imported into Matlab (2014b, Mathworks, USA), for further analysis. Mean peak-to-peak signal, noise and signal-to-noise ratio (SNR) were measured using custom-written scripts. Further metrics, such as CAPs per channel were also calculated and CAPs corresponding to the subsequent 'bursting' of activity from vagus nerve activity after IL-1β injection were isolated from the 200 Hz high passed signal.

Immunohistochemistry

Immunohistochemistry was used to assess tissue response to implanted microelectrodes. Under CO_2 anesthesia, mice were perfused with intracardial injection of 4% paraformaldehyde in phosphate buffered saline (PBS). Tissue samples were embedded in an optimal cutting temperature compound and frozen over dry ice. 10 μm sections were cut on a cryostat, mounted on slides (Superfrost, Thermo Fisher Scientific) and dried.

Slides were incubated for 30 min at room temperature in blocking buffer (5% normal horse serum, tris-buffered saline (TBS), 0.1% Tween 20) and then in 3% hydrogen peroxide solution for 15 min. Samples were stained with anti-CD3 antibody (500 A2, eBioscience, 1:75) and anti-I-Ab antibody (KH74, BD Pharmingen, 1:300). Primary antibodies were diluted in antibody diluent (5% normal horse serum, TBS, 0.1% Tween 20) overnight at 4 °C. The following day, after washing in wash buffer (TBS 0.1% Tween 20), anti-CD3 was incubated with anti-hamster biotinylated secondary antibody (1:200) diluted in antibody buffer and anti-I-Ab was incubated in antibody buffer for 30 min at room temperature. Diaminobenzidine (DAB, Vector Laboratories) followed by counterstaining with haematoxylin staining was used. Images were captured with a Leica Microsystems DMRB microscope.

Images were analysed in the Matlab environment (2014b Mathworks, USA) as previously described [17]. In brief, image intensities were normalized to the endogenous background staining for each slide. Radial distribution intensity measurements, centered on the nerve were measured concentrically, every 2 μm, with measurements obtained up to 150 μm from the identified nerve center.

Statistics

Data are expressed as mean $\pm$ SEM. Differences in cytokine levels between groups were analysed using unpaired two-tailed Student's t-test (Prism 7.0, GraphPad software, San Diego, CA, USA). Differences in radial distribution intensities were analysed using paired, two-tailed Student's t test. $p < 0.05$ was considered significant.

Results

Electrode impedance

Electrode impedance as measured at 1 kHz in physiological saline was 100 ± 12, 411 ± 21, and 910 ± 75 kΩ for 6400, 2500 and 225 μm^2 recording sites, respectively ($n = 320$ sites). The impedance values indicate that the microfabrication process between the different electrode designs was stable and consistent.

Vagus nerve recordings using microelectrodes capture high fidelity CAPs

A microelectrode was implanted around the left cervical vagus nerve in an anesthetized mouse and baseline activity recorded for 30 min (figure 2(A)). To investigate the maximal number of features obtainable by the recording electrodes, 50 μl of 4 mM KCl was applied directly on top of the vagus nerve to fully depolarise it (figure 2(B)). Parafilm was placed underneath the nerve before application to prevent the spread of KCl to surrounding structures. Data was acquired continuously for an additional 30 min after KCl application. We observed an increase in overall electrical activity and obtained a good number of CAPs across all recording channels (figure 2(C), Mean $\pm$ SEM CAPs $= 2.36 \pm 0.50$ per channel). Further, clear separation of CAPs were observed in the PCA space (data not shown). High fidelity signal (477 ± 38 μV)

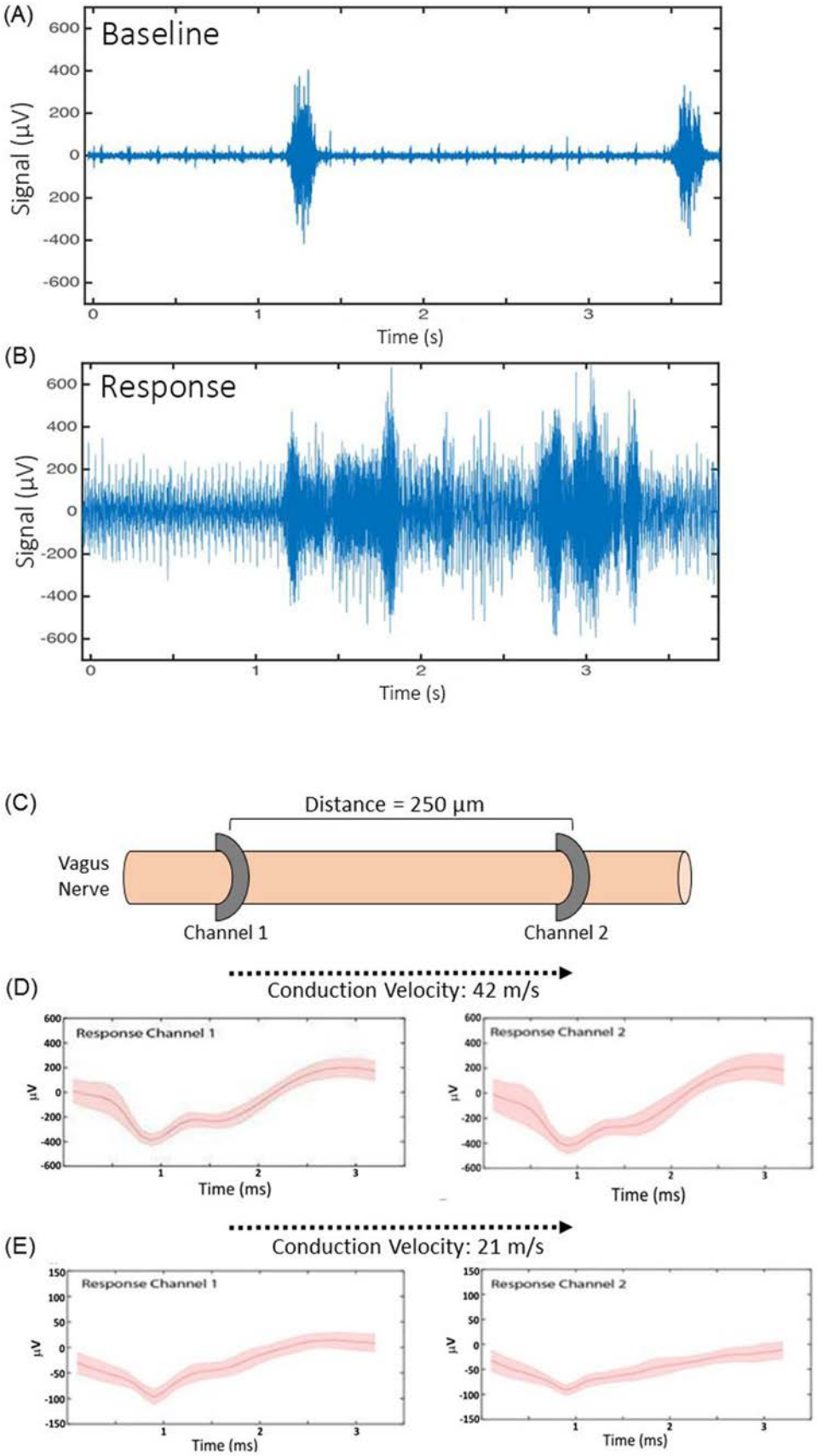

Figure 4. Electrical activity in response to interleukin-1β injection. (A) Baseline electrical activity in anesthetized mice recorded from a microelectrode on the left vagus nerve. (B) Electrical activity over a 3 s time period, 5 min after intraperitoneal injection of IL-1β. (C) Schematic of microelectrode placement along the cervical vagus nerve. (D) and (E) Features were extracted and CAPs isolated across multiple channels. Two examples are shown. The time delay in capturing these signal across the channels was used to calculate conduction velocity.

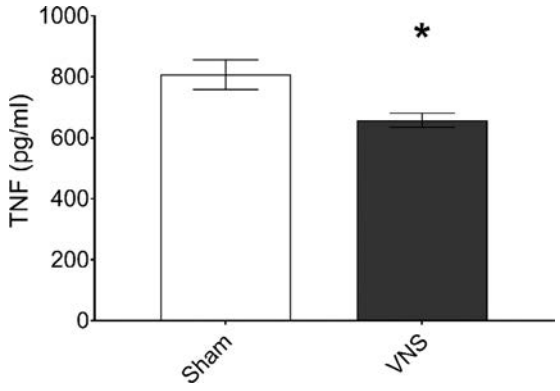

Figure 5. Vagus nerve stimulation in a mouse model of endotoxemia. Anesthetized mice were implanted with a microelectrode on the left cervical vagus nerve and electrical stimulation performed with the following settings: 1 mA output current, 250 μs biphasic pulse width, 50 μs interphase delay at a 10 Hz pulse frequency was applied across the two 80 $\times$ 80 microelectrode contact sites for 60 s and endotoxin injected intraperitoneally after 3 h of recovery. Serum was collected 90 min post-injection and TNFα was analysed by ELISA ($n = 30$, $^{*}p < 0.05$, unpaired, two-tailed, Student's *t*-test).

and SNR (8.63 $\pm$ 1.36) was obtained from the 2500 μm^2 sites (figure 2(D)). Good signal quality (179.5 $\pm$ 24.5 μV) and SNR (5.98 $\pm$ 0.81) with 3.25 $\pm$ 0.45 features per channel were obtained from the 6400^2 μm sites (figure 2(E)). The impedance of the 225 μm^2 sites was too high to allow for meaningful CAP isolation over the noise band (data not shown).

No change in vagus nerve activity observed upon saline challenge

In anesthetized mice implanted with a microelectrode on the left vagus nerve, 200 μl of saline was injected intraperitoneally during continuous electrophysiological acquisition. At the point of injection (time '0' s), an acute increase of activity lasting less than 3 s was observed. No change in amplitude and frequency of the recorded signal was observed after saline injection as compared to baseline, which was consistent across all animals. The electrical activity associated with the cardiac and respiratory cycles also remained unchanged (figure 3).

Vagus nerve CAPs associated with intraperitoneal injection of IL-1β Intraperitoneal injection of IL-1β in mice has been described to elicit an electrical response measurable by electrodes on the cervical vagus nerve [13]. Pharmacological challenges can evoke CAPS [20, 21]. The waveforms recorded from the surface electrodes in this study show distinct waveforms (triphasic, monophasic, biphasic) and time course (~3 ms) consistent with CAPs. To evaluate whether these microelectrodes are capable of capturing the CAPs elicited by IL-1β injection, a subset of mice were injected with IL-1β (350 ng per kg in 200 μl saline) intraperitoneally after a 30 min baseline recording (figure 4(A)). Compared with baseline, distinctive CAP shapes and interspike intervals were observed in the bursts 5 min after injection (figures 4(B)–(D)). These bursts were only found in a subset of the 14 adjacently arranged recording channels spaced 250 μm apart.

Recorded 'spike' times were used to calculate the delay between the specific features being picked up on the channels. This information enables calculation of the conduction velocity of the given features and deduction of the likely type of fibres involved in the response (figure 4(C)). For example, the difference between a burst-associated feature captured across two sites spaced 250 μm apart, was 6 ms. This corresponds to a conduction velocity of 42 m s^{-1}. Another feature captured across two channels had a 12 ms difference in times, which equates to a 21 m s^{-1} conduction velocity (figure 4(D)). The longitudinal configuration of the microelectrode also permits using spike times for specific features to determine directionality, i.e. whether a feature represents an efferent or afferent signal propagation. Thus, capturing burst-associated CAPs on multiple channels can be a tool to determine which fiber types are likely involved in a response.

Electrical stimulation of the cervical vagus nerve using the microelectrode reduced TNFα in endotoxemia

Vagus nerve stimulation of the cervical vagus nerve is known to reduce endotoxin-induced serum levels of TNFα by activating the inflammatory reflex [7, 18, 22]. To investigate whether this microelectrode design is capable of activating the inflammatory reflex, we studied vagus nerve stimulation in an established model of endotoxemia.

Mice were anesthetized and implanted with a microelectrode on the left cervical vagus nerve. Electrical stimulation through the microelectrode was applied for 60 s using the following settings: 1 mA output current, 250 μs biphasic pulse width duration, 50 μs interphase delay, at a 10 Hz pulse frequency. 3 h after this stimulation, 5 mg kg^{-1} endotoxin was injected intraperitoneally. Mice were euthanized 90 min later and serum collected and analysed for TNFα. The TNFα levels were significantly lower in the electrically stimulated mice as compared to sham-operated controls ($n = 30$; $p < 0.05$), validating the design capability to activate the inflammatory reflex [18] (figure 5).

Minimal foreign body response elicited by the implanted microelectrode

Anesthetized mice were implanted with a microelectrode on the left cervical vagus nerve. The left cervical vagus nerve along with surrounding tissues were harvested 12 weeks after implantation. Presence of CD3 and I-Ab, molecules associated with inflammation, was determined by immunohistochemistry. No significant differences in either CD3 or I-Ab staining were found between non-implanted and implanted nerve areas (figure 6) as determined by normalised radial distribution analysis extending 150 μm from the cross-sectional nerve center [17]. The limited inflammatory response observed indicates high biocompatibility of the implanted microelectrode.

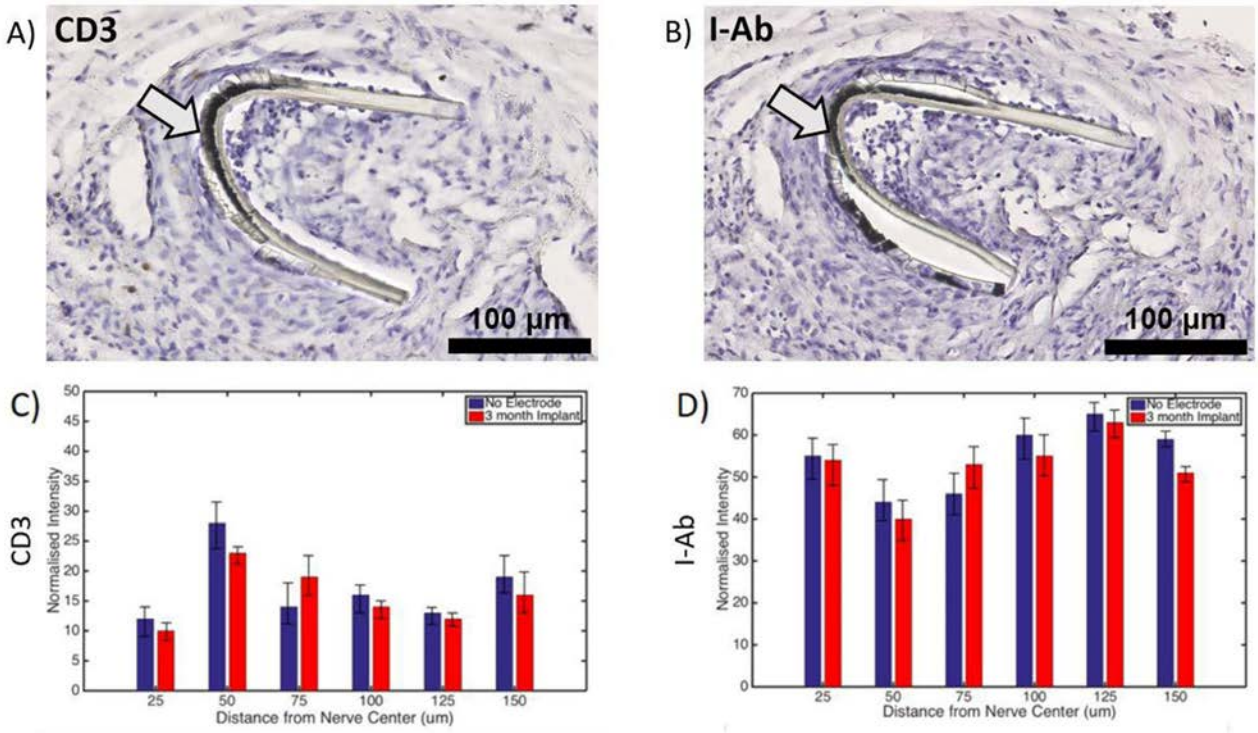

Figure 6. Limited inflammation at the microelectrode implantation site. Mice were implanted with a microelectrode on the left cervical vagus nerve. The tissue was collected 12 weeks later and stained using anti-CD3 and anti-I-Ab antibodies. Examples of images for (A) anti-CD3 and (B) anti-I-Ab staining are shown. Arrows point to electrode. Black scale bars depict 100 μm. No significant differences were found in the radial distribution of (C) anti-CD3 or (D) anti-I-Ab staining between the 12 week implanted site and the non-implanted site across 150 μm of the nerve diameter.

Discussion

Here, we present a novel, high density, customisable, 16 channel microelectrode intended for both acute and chronic stimulation and recording of the electrical activity in the mouse cervical vagus nerve. The microelectrode is based on thin film parylene-C technology, equipped with a ribbon cable, external connector and other features to facilitate secure positioning of the microelectrode *in vivo*.

The ultra-thin, inherently flexible, and customisable design of the microelectrode developed in this study allows for improved interfacing with small diameter peripheral nerves in mice and avoids the increased tissue pressure associated with bulky silicone cuffs. Although silicone based electrodes have been used successfully in rats [32], and in humans [33–36], the inherent minute size and manipulation of the nerve, make it difficult for such a strategy to be employed chronically in mice. In addition, nerve electrodes implanted in previous studies have often induced inflammation around the nerve causing device degradation and failure, limiting the functionality in small animals due to mechanical damage and nerve injury [14]. In contrast, our chronic microelectrode implantation showed a minimal foreign body response over a 12 week period.

The microelectrode in this study was evaluated for recording and stimulation performance in mice, showing good feature detection during specific challenges (e.g. KCl and IL-1β) and effective stimulation compared to sham-operated controls as shown in the well-characterized model of endotoxemia [9, 22]. The reduction in TNFα in response to electrical vagus nerve stimulation is consistent with prior studies, and validates the stimulation capability of the microelectrode [7, 22]. Thus, this new technology promises to enable the study of inflammatory reflex activation in acute and chronic disease models in mice for extended periods of time [3, 9].

The unipolar recording setup using the microelectrode for the vagus nerve obtained high fidelity signals in response to a KCl challenge. A unipolar recording setup was used in order to determine the signal propagation velocities from the mouse cervical vagus nerve, which would be difficult in other recording setups that would require larger exposure of the nerve in an otherwise limited surgical field.

A contributing factor to the high fidelity recordings was likely excellent adhesion to the nerve, of this microelectrode of flexible parylene-C, [23] thereby increasing the electrical coupling for the recording sites. Previous studies of peripheral implants used for rodents have reported peak-to-peak signal amplitudes ranging from 100–900 μV in response to electrical stimuli [24–29]. In this study, recorded peak-to-peak signal amplitudes ranged between 100 and 2500 μV in response to pharmacological stimuli, and differed with the size of recording sites.

The recording from multiple channels configured in close proximity along and around the nerve enabled the observation that some isolated features were detected on some but not all channels, i.e detectable only in specific locations on the nerve. Using bipolar electrodes, Steinberg *et al* [13] recently

demonstrated cytokine-specific neurograms in the sensory vagus nerve in mice. In light of this, it is tempting to speculate that the multichannel microelectrode technology presented here could be used to improve resolution for detection of specific signatures of inflammation. The current device design is fabricated with 16 channels, but it can easily be scaled up to ~1000 channels with the use of previously established process flows [30]. We find it plausible that a high density electrode array would significantly improve interface performance.

Capturing multiple features across different channels allowed observation of the delay between channels of specific features, information that subsequently was used to calculate conduction velocities and directionality for propagation. Different fibre types in the peripheral nervous system are associated with specific conduction velocities [31, 32]. Hence, information on signal propagation velocities may identify specific fibre types involved in a response, and indicate whether the activity is efferent or afferent.

The histological analysis indicates that this microelectrode may be suitable for chronic implantation with limited risk for nerve damage, a considerable challenge for chronic interfacing. This is perhaps attributable to the multiple design measures to prevent unnecessary tethering stresses on the nerve—ultra-thin film design, necking region to decouple the ribbon cable from the microelectrode, and an incorporated ribbon cable to allow for stabilisation of the connector on the skull of the mouse.

The ability to combine effective simulation, high fidelity recording and chronic implantation in a single device, as we have shown, is potentially very useful for studying mechanisms and physiological effects of inflammatory reflex activation in a multiplicity of genetically modified mice. Chronic implantation may allow for repeated acquisition of electrical signatures potentially associated with specific disease activity and, combined with stimulation, theoretically enables design of closed-loop systems for automated correction of aberrant activity through electrical nerve stimulation. Studies are ongoing to further characterise the recording and stimulation performance of the microelectrode in chronic mouse model settings.

Conclusions

Here, we present a novel, flexible, biocompatible, high channel count, cuff-like microelectrode designed for acute and chronic stimulation and recording of the mouse cervical vagus nerve. This technology aims to improve our ability to mechanistically dissect the neurophysiology and molecular biology of the reflex control of inflammation and provide stepping stones for the advancement of bioelectronic medicine.

Acknowledgments

We would like to thank Emily Battinelli and Dr Valentin Pavlov at the Feinstein Institute for Medical Research, Manhasset, New York, USA for valuable input. This work was supported in part by NIH Director's Pioneer Award 1DP1NS087724, NIH 1R24MH106075, NIH 1R01MH103910, NIH 1R01EY023173, Knut and Alice Wallenberg's Foundation 20140212, Heart Lung Foundation 20150767, and the New York Stem Cell Foundation Robertson Award.

References

[1] Tracey K J 2015 Shock medicine *Sci. Am.* **312** 28–35
[2] Chow B Y and Boyden E S 2013 Optogenetics and translational medicine *Sci. Transl. Med.* **5** 177ps5
[3] Bonaz B, Sinniger V and Pellissier S 2016 Anti-inflammatory properties of the vagus nerve: potential therapeutic implications of vagus nerve stimulation *J. Physiol.* **594** 5781–90
[4] Tracey K J 2016 Reflexes in immunity *Cell* **164** 343–4
[5] Pavlov V A and Tracey K J 2017 Neural regulation of immunity: molecular mechanisms and clinical translation *Nat. Neurosci.* **20** 156–66
[6] Tracey K J 2002 The inflammatory reflex *Nature* **420** 853–9
[7] Borovikova L V *et al* 2000 Vagus nerve stimulation attenuates the systemic inflammatory response to endotoxin **405** 458–62
[8] Olofsson P S, Rosas-Ballina M, Levine Y A and Tracey K J 2012 Rethinking inflammation: neural circuits in the regulation of immunity *Immunol. Rev.* **248** 188–204
[9] Koopman F A *et al* 2003 Vagus nerve stimulation inhibits cytokine production and attenuates disease severity in rheumatoid arthritis *Proc. Natl Acad. Sci. USA* **113** 8284–9
[10] Bonaz B, Sinniger V, Hoffmann D and Clarenc D 2016 Chronic vagus nerve stimulation in Crohn's disease: a 6-month follow-up pilot study *Neurogastroenterol. Motil.* **28** 948–53
[11] Watkins L R *et al* 1995 Blockade of interleukin-1 induced hyperthermia by subdiaphragmatic vagotomy: evidence for vagal mediation of immune-brain communication *Neurosci. Lett.* **183** 27–31
[12] Niijima A 1996 The afferent discharges from sensors for interleukin 1 beta in the hepatoportal system in the anesthetized rat *J. Auton. Nerv. Syst.* **61** 287–91
[13] Steinberg B E *et al* 2016 Cytokine-specific neurograms in the sensory vagus nerve *Bioelectron. Med.* **3** 7–17
[14] Loeb G E and Peck R A 1996 Cuff electrodes for chronic stimulation and recording of peripheral nerve activity *J. Neurosci. Methods* **64** 95–103
[15] Sohal H S *et al* 2014 The sinusoidal probe: a new approach to improve electrode longevity *Front. Neuroeng.* **7** 10
[16] Sohal H S, Konstantin V, Andrew J, Baker S N and Anthony O 2016 Design and microfabrication considerations for reliable flexible intracortical implants *Front. Mech. Eng. China* **2**
[17] Sohal H S, Clowry G J, Jackson A, O'Neill A and Baker S N 2016 Mechanical flexibility reduces the foreign body response to long-term implanted microelectrodes in rabbit cortex *PLoS One* **11** e0165606
[18] Pavlov V A, Wang H, Czura C J, Friedman S G and Tracey K J 2003 The cholinergic anti-inflammatory pathway: a missing link in neuroimmunomodulation *Mol. Med.* **9** 125–34
[19] Quiroga R Q, Nadasdy Z and Ben-Shaul Y 2004 Unsupervised spike detection and sorting with wavelets and superparamagnetic clustering *Neural. Comput.* **16** 1661–87
[20] Niijima A 1982 Glucose-sensitive afferent nerve fibers in the hepatic branch of the vagus nerve in the guinea-pig *J. Physiol.* **332** 315–23
[21] Niijima A and Meguid M M 1994 Parenteral nutrients in rat suppresses hepatic vagal afferent signals from portal vein to hypothalamus *Surgery* **116** 294–301

[22] Olofsson P S, Levine Y A, Caravaca A, Chavan S, Pavlov V A, Faltys M and Tracey K J 2015 Single-pulse and unidirectional electrical activation of the cervical vagus nerve reduces tumor necrosis factor in endotoxemia *Bioelectron. Med.* **2** 37–42

[23] Seymour J P, Elkasabi Y M, Chen H-Y, Lahann J and Kipke D R 2009 The insulation performance of reactive parylene films in implantable electronic devices *Biomaterials* **30** 6158–67

[24] Yu H, Xiong W, Zhang H, Wang W and Li Z 2014 A cable-tie-type parylene cuff electrode for peripheral nerve interfaces *2014 IEEE 27th Int. Conf. on Micro Electro Mechanical Systems (MEMS)*

[25] Lee S *et al* 2016 Flexible epineural strip electrode for recording in fine nerves *IEEE Trans. Biomed. Eng.* **63** 581–7

[26] Badia J, Raspopovic S, Carpaneto J, Micera S and Navarro X 2016 Spatial and functional selectivity of peripheral nerve signal recording with the transversal intrafascicular multichannel electrode (TIME) *IEEE Trans. Neural Syst. Rehabil. Eng.* **24** 20–7

[27] Lee S *et al* 2016 Selective stimulation and neural recording on peripheral nerves using flexible split ring electrodes *Sensors Actuators* B **242** 1165–70

[28] Seo D *et al* 2016 Wireless recording in the peripheral nervous system with ultrasonic neural dust *Neuron* **91** 529–39

[29] Kagaya M, Lamb J, Robbins J, Page C P and Spina D 2002 Characterization of the anandamide induced depolarization of guinea-pig isolated vagus nerve *Br. J. Pharmacol.* **137** 39–48

[30] Harper A A and Lawson S N 1985 Electrical properties of rat dorsal root ganglion neurones with different peripheral nerve conduction velocities *J. Physiol.* **359** 47–63

[31] Steffens H, Dibaj P and Schomburg E D 2012 *In vivo* measurement of conduction velocities in afferent and efferent nerve fibre groups in mice *Physiol. Res.* **61** 203–14

[32] Tyler D J and Durand D M 2003 Chronic response of the rat sciatic nerve to the flat interface nerve electrode *Ann. Biomed. Eng.* **31** 633–42

[33] Graczyk E L, Schiefer M A, Saal H P, Delhaye B P, Bensmaia S J and Tyler D J 2016 The neural basis of perceived intensity in natural and artificial touch *Sci. Transl. Med.* **8** 362ra142

[34] Schiefer M A *et al* 2013 Selective activation of the human tibial and common peroneal nerves with a flat interface nerve electrode *J. Neural Eng.* **10** 056006

[35] Schiefer M A, Tyler D J and Triolo R J 2012 Probabilistic modeling of selective stimulation of the human sciatic nerve with a flat interface nerve electrode *J. Comput. Neurosci.* **33** 179–90

[36] Fisher L E, Tyler D J, Anderson J S and Triolo R J 2009 Chronic stability and selectivity of four-contact spiral nerve-cuff electrodes in stimulating the human femoral nerve *J. Neural Eng.* **6** 046010